Science Translational Medicine AAAS

CD44-SLC1A2 Gene Fusions in Gastric Cancer

Jiong Tao *et al.*
Sci Transl Med **3**, 77ra30 (2011);
DOI: 10.1126/scitranslmed.3001423

Editor's Summary

Bad Drivers Steer Scientists Toward New Drug Targets

It's ironic, but cancer cells are notoriously bad at cell division, losing bits and rearranging chunks of the genome in the process. One result of this chaos is the birth of chimeric genes, wherein one gene segment gets erroneously fused to part of another, sometimes forming peculiar hybrid proteins that contribute to the cancer cell phenotype. For example, the fused aberrant *BCR-ABL* gene drives chronic myelogenous leukemia and has proven to be a vulnerable target for therapy. Gene fusions in solid cancers are not so easy to spot, but have been located in prostate and small cell lung cancers. Now, Tao and her co-workers have documented a fusion gene that forms in a small percentage of gastric tumor cells and may contribute to the development of cancer.

The authors analyzed copy number variations of genes in more than 100 primary gastric tumors and 27 established gastric tumor cell lines and pinpointed a common breakpoint in three and one, respectively. The resulting chimeric gene fused most of the coding region of *SLC1A2/EAAT2* (which encodes a glutamate transporter) to what is probably the strong transcriptional promoter of its neighboring gene, *CD44*, likely the result of a chromosome inversion. The fusion gene generated a truncated SLC1A2 protein in the original tumors and in a new group of gastric cancers created by the authors through overexpression of the fusion gene in normal gastric cells.

But an abnormal protein that lives in tumor cells can be an innocent bystander. So, the authors asked whether the truncated SLC1A2 contributes to gastric cancer development, and their evidence suggested that the answer is yes. Cells in which shortened SLC1A2 expression was silenced with small interfering RNA were less proficient at dividing and invading soft substrates —hallmarks of cancer cells—and overexpression of the pruned protein enhanced these traits. Consistent with the function of SLC1A2 as a transporter of glutamate, the amino acid —which can act as a growth regulator —existed in higher concentrations in gastric cancer cells and cell lines than in normal cells. And in a final set of incriminating evidence, tumor cells that sported the *CD44-SLC1A2* fusion gene had higher amounts of SLC1A2 than did wild-type cells, suggesting that this aberrant protein may trigger a pro-oncogenic phenotype.

Most other genes that are fused in cancers encode kinase enzymes or transcriptional regulatory proteins. The implication of an overexpressed metabolism-related gene in some gastric tumors may define a new class of cancer-driving genes, although the protein could also augment other cancer-promoting genetic aberrations. The utility of this fusion gene as a drug target or prognostic tool will require more studies, but this particular mistake made by a dividing cancer cell may act as a GPS that directs researchers down a new therapeutic avenue for gastric cancer.

Science Translational Medicine (print ISSN 1946-6234; online ISSN 1946-6242) is published weekly, except the last week in December, by the American Association for the Advancement of Science, 1200 New York Avenue NW, Washington, DC 20005.

CANCER

CD44-SLC1A2 Gene Fusions in Gastric Cancer

Jiong Tao,[1,2] Nian Tao Deng,[2] Kalpana Ramnarayanan,[3] Baohua Huang,[1] Hue Kian Oh,[3] Siew Hong Leong,[4] Seong Soo Lim,[5] Iain Beehuat Tan,[2,6] Chia Huey Ooi,[2] Jeanie Wu,[3] Minghui Lee,[3] Shenli Zhang,[2] Sun Young Rha,[7] Hyun Cheol Chung,[7] Duane T. Smoot,[8] Hassan Ashktorab,[8] Oi Lian Kon,[4] Valere Cacheux,[5] Celestial Yap,[1] Nallasivam Palanisamy,[5]* Patrick Tan[1,2,3,5,9]†

Fusion genes are chimeric genes formed in cancers through genomic aberrations such as translocations, amplifications, and rearrangements. To identify fusion genes in gastric cancer, we analyzed regions of chromosomal imbalance in a cohort of 106 primary gastric cancers and 27 cell lines derived from gastric cancers. Multiple samples exhibited genomic breakpoints in the 5′ region of *SLC1A2/EAAT2*, a gene encoding a glutamate transporter. Analysis of a breakpoint-positive SNU16 cell line revealed expression of a *CD44-SLC1A2* fusion transcript caused by a paracentric chromosomal inversion, which was predicted to produce a truncated but functional *SLC1A2* protein. In primary tumors, *CD44-SLC1A2* gene fusions were detected in 1 to 2% of gastric cancers, but not in adjacent matched normal gastric tissues. When we specifically silenced *CD44-SLC1A2*, cellular proliferation, invasion, and anchorage-independent growth were significantly reduced. Conversely, *CD44-SLC1A2* overexpression in gastric cells stimulated these pro-oncogenic traits. *CD44-SLC1A2* silencing caused significant reductions in intracellular glutamate concentrations and sensitized SNU16 cells to cisplatin, a commonly used chemotherapeutic agent in gastric cancer. We conclude that fusion of the *SLC1A2* gene coding region to *CD44* regulatory elements likely causes *SLC1A2* transcriptional dysregulation, because tumors expressing high *SLC1A2* levels also tended to be *CD44-SLC1A2*–positive. *CD44-SLC1A2* may represent a class of gene fusions in cancers that establish a pro-oncogenic metabolic milieu favoring tumor growth and survival.

INTRODUCTION

Gastric adenocarcinoma, or gastric cancer (GC), is a leading cause of global cancer mortality, with a 5-year survival rate of ~20% (*1*, *2*). Particularly prevalent in several Asian countries (*3*), most GC patients present with advanced-stage disease, although in Japan and Korea screening programs with barium photofluorography or endoscopy allow earlier detection (*4*, *5*). Current strategies for treating GC patients are far from optimal, with conventional surgery and chemotherapy regimens conferring modest survival benefits and median survival times of 7 to 10 months (*6*).

Clinical risk factors for GC include a high-salt diet, *Helicobacter pylori* infection, and smoking (*2*). Although familial patterns of GC incidence have been reported, most GC cases are sporadic. Studies investigating the genetic basis of GC have identified germline polymorphisms in cytokine genes (for example, *interleukin 1*β and *TLR4*) (*7*, *8*) and mutations in cell junction genes (CDH1) as inherited GC risk factors (*9*). In gastric tumors, somatic mutations in oncogenes and tumor suppressor genes such as *p53*, *RUNX3*, and β-*catenin* have been reported (*10*–*12*), along with signature genomic amplifications (7q, 8p, 17q, and 20q) and deletions (5q, 6p, and 18q) (*13*). Identifying additional molecular aberrations in GC could provide further mechanistic insights into GC pathogenesis and highlight opportunities for early detection and new therapies.

Fusion genes are hybrid genes formed by the combination of two normally separate and distinct genes. In cancers, fusion genes can be produced by genomic amplifications, translocations, and rearrangements (*14*), resulting in juxtaposition of oncogenic proteins with strong promoters (for example, *IgH-Myc*) (*15*) or chimeric proteins with oncogenic signaling potential (for example, *BCR-ABL*) (*16*). Because of their cancer-specific nature, fusion genes have the potential to act as useful diagnostic and therapeutic targets. To date, the vast majority of cancer-related fusion genes have been identified primarily in hematological malignancies, where they have been used to identify particular cancer subtypes (for example, *PML-RAR*α in acute promyelocytic leukemia) and used as drug targets [for example, *BCR-ABL* in chronic myelogenous leukemia (CML)] (*17*, *18*).

In contrast to the hematological malignancies, in solid epithelial cancers, very few fusion genes have been identified. In these cancers, higher genomic complexity and clonal heterogeneity can confound standard cytogenetic assays (*19*). Nevertheless, recent discoveries of *TMPRSS2-ERG* in prostate cancer (*20*) and *EML4-ALK* in non–small cell lung cancer (*21*) have confirmed the existence of recurrent fusion genes in solid tumors and shown that these can be identified with high-resolution genomic approaches. Previously, we have used transcriptome sequencing to identify *BRAF*-related gene fusions in GC, providing evidence for this important class of molecular aberrations in gastrointestinal (GI) cancers (*22*). Here, we adopted an alternative strategy to discover a recurrent fusion gene in GC.

[1]Department of Physiology, Yong Loo Lin School of Medicine, National University of Singapore, 5 Lower Kent Ridge Road, Singapore 119074, Singapore. [2]Cancer and Stem Cell Biology, Duke-NUS Graduate Medical School, 8 College Road, Singapore 169857, Singapore. [3]Cellular and Molecular Research, National Cancer Centre of Singapore, 11 Hospital Drive, Singapore 169610, Singapore. [4]Division of Medical Sciences, National Cancer Centre of Singapore, Singapore 169610, Singapore. [5]Genome Institute of Singapore, 60 Biopolis Street, Genome 02-01, Singapore 138672, Singapore. [6]Division of Medical Oncology, National Cancer Centre of Singapore, Singapore 169610, Singapore. [7]Department of Internal Medicine, Yonsei Cancer Center, Yonsei University College of Medicine, 134 Shinchon-Dong, Seodaemun-Ku, Seoul 120-752, South Korea. [8]Department of Medicine and Cancer Center, Howard University College of Medicine, 2041 Georgia Avenue, Washington, DC 20060, USA. [9]Cancer Science Institute of Singapore, Yong Loo Lin School of Medicine, National University of Singapore, Singapore 119074, Singapore.
*Present address: Michigan Center for Translational Pathology and Department of Pathology, University of Michigan, Ann Arbor, MI 48109, USA.
†To whom correspondence should be addressed. E-mail: gmstanp@duke-nus.edu.sg

RESULTS

Analysis of GC copy number alterations identifies recurrent *SLC1A2/EAAT2* genomic breakpoints

We hypothesized that a detailed fine-scale survey of genomic copy number alterations (CNAs) in GC might reveal potential genes disrupted by fusion events. Using high-density array-based comparative genomic hybridization (aCGH) microarrays, we profiled a discovery cohort of 133 GCs (106 primary tumors and 27 cell lines). In a validation of the aCGH data, we successfully reidentified several previously described genomic aberrations in GC, including amplifications in *c-Myc* (*23*), *HER2* (*24*), *RAB23* (*25*), and *PTEN* deletions (*26*) (fig. S1). To nominate potential fusion genes, we used a technique called genomic breakpoint analysis (GBA), previously used to identify fusion genes in leukemia (*27*). In this strategy, putative chromosomal breakpoints were identified by examining closely spaced microarray probes displaying prominent transitions in copy number status, from low to high copy number or vice versa. Figure 1A provides a representative example of a genomic breakpoint in the *CALCR* gene. In total, we identified 99 genomic breakpoints occurring in genes such as *CALCR*, *PERLD1*, and *CKAP5* (table S1).

For most genes exhibiting genomic breakpoints in multiple samples (for example, *CRKRS* and *TTC25*), the breakpoints were randomly scattered throughout the gene body, consistent with a random breakage during chromosomal amplification. However, 4 of 133 GCs (three primary tumors and one cell line—GC980417, GC20021048, GC2000038, and SNU16) exhibited genomic breakpoints specifically localized to the 5′ region of the *SLC1A2/EAAT2* gene, encoding a high-affinity glutamate transporter (hereafter referred to as *SLC1A2*) (Fig. 1B). To validate the *SLC1A2* breakpoint region, we performed fluorescence in situ hybridization (FISH) analysis using fosmid probes that mapped upstream or downstream of the putative breakpoint (WI2-67O19 and WI2-1928P9). Supporting the aCGH data, the WI2-67O19 upstream probe (35384118-35427600) covering the first exon of *SLC1A2* showed three to four signals in SNU16 nuclei (Fig. 1C, left), confirming previous studies that SNU16 is a naturally tetraploid cell line (*28*). In contrast, the downstream WI2-1928P9 probe (35323126-35359663) located at *SLC1A2* intron 1 showed multiple hybridization signals (>50 copies), indicating a large amplification event (Fig. 1C, right).

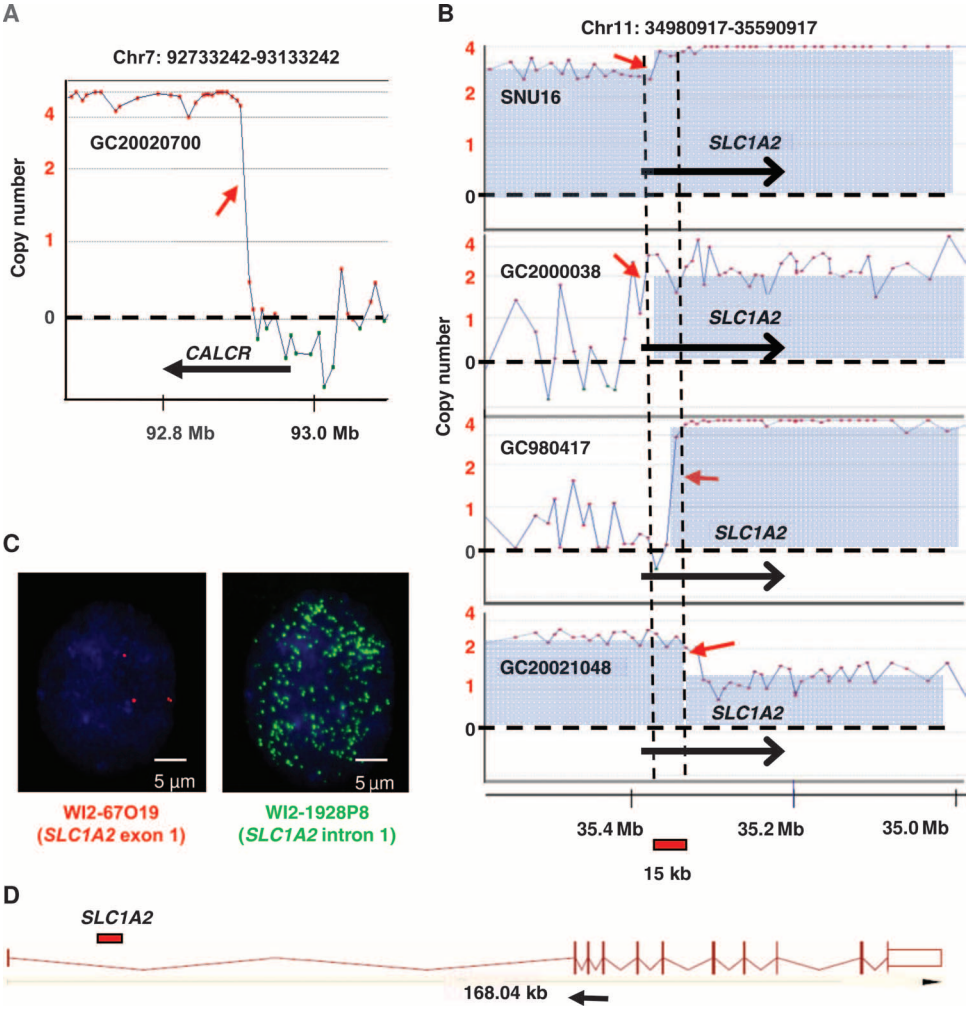

Fig. 1. Genomic breakpoint analysis of gastric cancer. (**A**) Representative example of a genomic breakpoint. aCGH profile of gastric cancer (GC) tumor GC20020700 exhibiting a genomic breakpoint in the *CALCR* gene on chromosome 7q12. *X* axis, physical chromosomal coordinates; *y* axis, $\log_2$-transformed smoothened values (that is, dotted line at 0 indicates copy number equal to 2). Red arrow, breakpoint of interest; dot, a microarray probe. (**B**) Genomic breakpoints in the 5′ region of *SLC1A2* in four GCs (three primary tumors and one cell line: GC2000038, GC980417, GC20021048, and SNU16). Red arrows, breakpoints of interest. (**C**) FISH validation of *SLC1A2* breakpoints. Probes WI2-67O19 (red) and WI2-1928P9 (green) cover *SLC1A2* exon 1 or intron 1, respectively. (**D**) Genomic organization of the *SLC1A2* gene. Vertical bars represent *SLC1A2* exons connected by intervening introns. Total length of the *SLC1A2* gene is 168 kb. Red bar, minimal common recurrent breakpoint region in *SLC1A2* intron 1 (15 to 24 kb); black arrow, location of oligonucleotide primer used for 5′ RLM-RACE analysis.

SLC1A2 breakpoint characterization reveals a *CD44-SLC1A2* gene fusion

Integrating the *SLC1A2* breakpoint regions from the aCGH and the FISH data, we defined a 15- to 24-kb minimal common breakpoint window in the *SLC1A2* first intron (Fig. 1, B and D, red bar). We hypothesized that chromosomal aberrations affecting this region might disrupt the *SLC1A2* gene and result in potential fusion partners. To test this possibility, we performed 5′ RNA ligase–mediated rapid amplification of complementary DNA (cDNA) ends (RLM-RACE) to characterize *SLC1A2* transcript sequences upstream of *SLC1A2* exon 2. A 250–base pair (bp) 5′ RACE product was identified in breakpoint-positive SNU16 cells, but not in other GC

cell lines without *SLC1A2* breakpoints (AGS, YCC1, YCC9, and N87) (Fig. 2A). Sequencing of the amplified SNU16 product revealed a *CD44-SLC1A2* fusion transcript, formed by the juxtaposition of *CD44* exon 1 to *SLC1A2* exon 2 (Fig. 2B). Complementary to the 5′ RACE analysis, a 3′ RACE analysis in SNU16 cells that characterized transcripts downstream of *SLC1A2* exon 1 did not identify any additional fusion partners besides wild-type *SLC1A2* transcripts (fig. S2A). To validate the 5′ RACE results, we designed combination sets of polymerase chain reaction (PCR) primers targeting *CD44* exon 1 (forward primer) and *SLC1A2* exons 3 to 6 (reverse primers) to directly detect the fusion by reverse transcription–PCR (RT-PCR). *CD44-SLC1A2* transcripts were detected in SNU16 cells, but not in other cell lines or in commercially available normal gastric (NG) tissue (Fig. 2C and fig. S2B). We confirmed expression of a complete ~1.6-kb *CD44-SLC1A2* transcript in SNU16 cells using RT-PCR primers targeting *CD44* exon 1 and *SLC1A2* exon 11 (the last *SLC1A2* exon) (fig. S2C). These results demonstrate the existence of a *CD44-SLC1A2* gene fusion in SNU16 cells.

CD44 and *SLC1A2* lie adjacent to each other on chromosome 11p13, being separated by only ~19 kb (Fig. 2D). The two genes are transcribed toward each other, indicating that they have distinct promoters. Because they lie on opposite strands, it is unlikely that the *CD44-SLC1A2* fusion is caused by a transcriptional readthrough event (*29*). We thus hypothesized that the *CD44-SLC1A2* gene fusion might have been caused by a paracentric chromosomal inversion (fig. S3A). Notably, 11p13-15, where *CD44* and *SLC1A2* are located, has been described as a frequent site of genome rearrangement in gastric and esophageal cancers (*30*). Spectral karyotyping (SKY) analysis confirmed the presence of at least two 11p13-11p14 genome rearrangements in SNU16 cells: one involving fusion of chromosome 1 with chromosome 11 at band 11p13-14 and the second involving a complex chromosomal scenario with rearrangements joining chromosomes 5, 10, and 11 (fig. S3B).

We used two different strategies to verify the presence of *CD44/SLC1A2* genomic inversions in this region. First, we used fiber-FISH, a high-resolution method for genomic DNA mapping (*31*). Fosmid

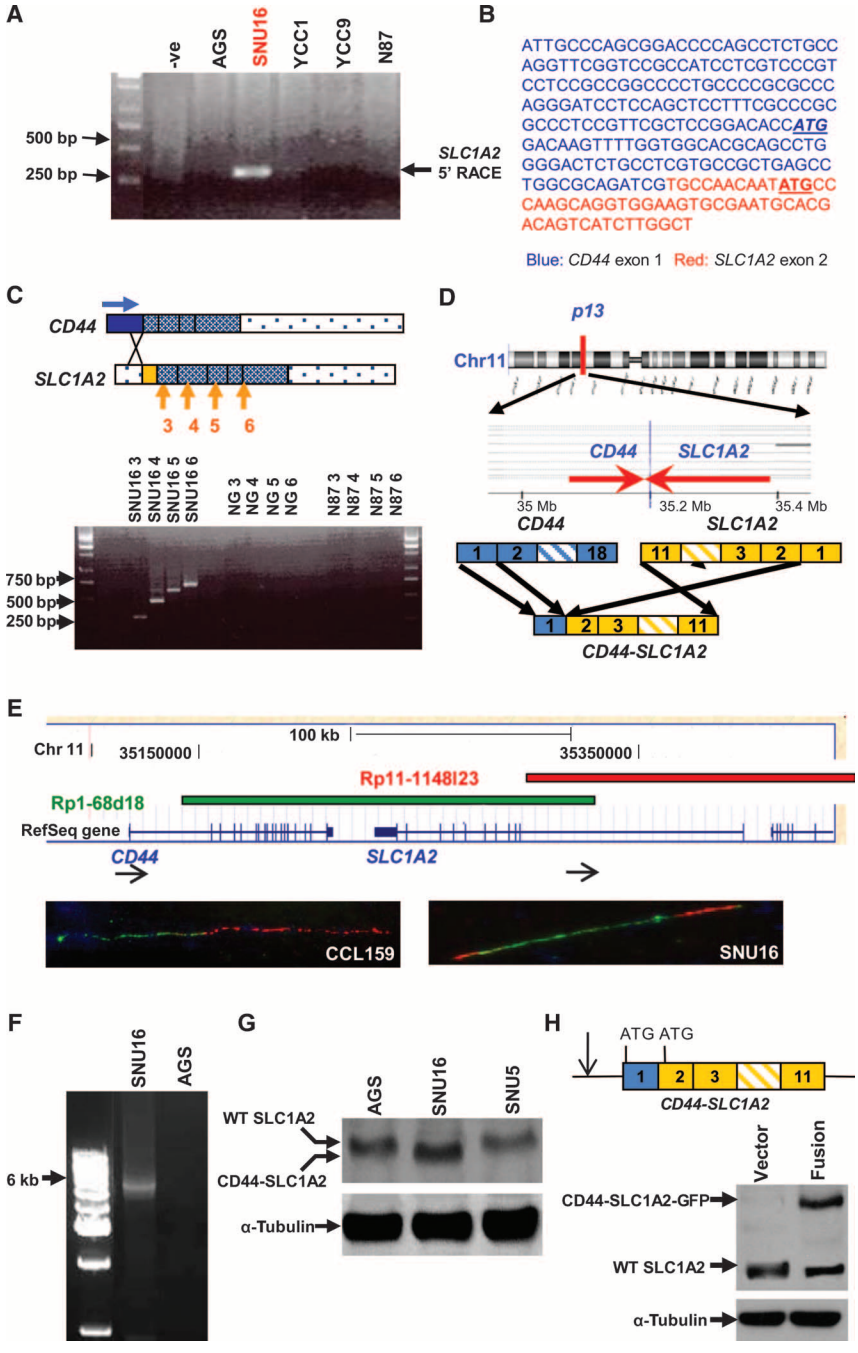

Fig. 2. *CD44-SLC1A2* gene fusions. (**A**) 5′ *SLC1A2* RLM-RACE of GC cell lines. (**B**) *CD44-SLC1A2* fusion sequence. Blue, *CD44* exon 1; red, *SLC1A2* exon 2; underline, ATG sites. (**C**) *CD44-SLC1A2* RT-PCR. Primers were targeted to *CD44* exon 1 (blue arrow) and *SLC1A2* exons 3 to 6 (orange arrows). NG, normal stomach; N87, fusion-negative line. (**D**) Top: *CD44* and *SLC1A2* chromosomal organization. Bottom: *CD44-SLC1A2* relationship to *CD44* and *SLC1A2* parent genes. (**E**) Fiber-FISH. Top: Probe 1 (Rp1-68d18) covers *CD44* (3′ of intron 1) and *SLC1A2* (3′ of intron 1). Probe 2 (Rp11-1148I23) covers the 5′ region of *SLC1A2* intron 1 and upstream sequence. Bottom: Fiber-FISH images of control CCL159 cells and fusion-positive SNU16 cells. (**F**) Long-range PCR. Primers were targeted to *CD44* exon 1 and the *SLC1A2* first intron [black arrows in (E)]. SNU16, fusion-positive; AGS, fusion-negative. Primers are black arrows in (E). (**G**) Western blot of fusion-positive SNU16 and fusion-negative AGS and SNU5 cells (membrane fractions). Top: Anti-SLC1A2 antibodies. Bottom: α-Tubulin antibody control. (**H**) *CD44-SLC1A2* ectopic expression. Top: *CD44-SLC1A2* expression construct carrying a GFP tag. Arrow, promoter. ATG sites in *CD44* exon 1 and *SLC1A2* exon 2 are shown. Bottom: Immunoblotting with anti-SLC1A2 antibodies.

probes Rp1-68d18 (35146316-35329998, covering the *CD44* gene and a portion of the *SLC1A2* gene) and Rp11-1148l23 (35294107-35461767, covering the *SLC1A2* gene only) were hybridized to SNU16 cells or normal lymphoblastoid CCL159 cells. In the control CCL159 cells, we observed a normal chromosome as indicated by two distinct red and green probe signals lying adjacent to one another. In contrast, we detected in SNU16 cells a "split-apart" red-green-red signal, consistent with an inversion event occurring between these probes (Fig. 2E). Second, we directly confirmed a *CD44/SLC1A2* genomic inversion in SNU16 cells using long-range genomic PCR, followed by end-sequencing of the PCR products. Using primers located to *CD44* exon 1 and the *SLC1A2* first intron (black arrows in Fig. 2E), we successfully PCR-amplified and sequence-validated a *CD44-SLC1A2* inversion product in SNU16 fusion-positive cells but not in AGS cells (Fig. 2F). Collectively, these two alternative methods confirm the presence of a chromosomal inversion event in SNU16 cells between *CD44* and *SLC1A2*.

Sequence analysis of the *CD44-SLC1A2* fusion revealed two distinct protein translation patterns (fig. S4A). First, translation initiating from an ATG site in *CD44* exon 1 could produce a 65–amino acid protein, comprising 22 amino acids of *CD44* and 43 amino acids of novel sequence. Second, protein translation might also initiate from an alternative ATG site in *SLC1A2* exon 2, downstream of the fusion site. Translation from this alternative ATG would produce a 565–amino acid–long truncated *SLC1A2* protein, which is 17 amino acids shorter than the full-length form, but retaining all functionally relevant domains including transmembrane helices and symporter domains.

To test whether *CD44-SLC1A2* might produce a truncated SLC1A2 protein, we performed Western blotting using anti-SLC1A2 antibodies on fusion-positive and -negative GC cells. In SNU16 fusion-positive cells, we detected a smaller-sized SLC1A2 protein compared to fusion-negative AGS and SNU5 cells (Fig. 2G), consistent with translation initiating from *SLC1A2* exon 2 in SNU16 cells. To further demonstrate that the alternative ATG in *SLC1A2* exon 2 is capable of initiating protein translation, we cloned and expressed the full-length *CD44-SLC1A2* fusion gene in HFE145 gastric cells (*32*). Western blotting analysis confirmed expression of an immunoreactive SLC1A2 product in *CD44-SLC1A2*–transfected HFE145 cells of the expected size (Fig. 2H). This result demonstrates that the alternative ATG in *SLC1A2* exon 2 is sufficient to initiate translation.

CD44-SLC1A2 gene fusion is expressed in primary gastric cancers

To test whether *CD44-SLC1A2* is expressed in clinical specimens, we screened two of the three original index cases exhibiting *SLC1A2* genomic breakpoints (Fig. 1B). The third index tumor, GC20021048, had insufficient material available for analysis. *CD44-SLC1A2* expression was detected in tumor GC2000038, but not in corresponding matched normal tissue (Fig. 3A). This result demonstrates that *CD44-SLC1A2* expression can occur in primary tumors and that it is not a "private" event confined to SNU16 cells alone.

We then performed *CD44-SLC1A2* RT-PCR screening in an independent panel of 43 gastric tumors and matched gastric normal tissues. Two additional tumors that expressed the *CD44-SLC1A2* fusion transcript were identified (Fig. 3B). Similar to the index samples, *CD44-SLC1A2* was not expressed in corresponding matched normal samples (Fig. 3B, bottom), supporting the cancer-specific nature of the fusion transcript. Subsequent cloning and sequencing of *CD44-SLC1A2* in the fusion-positive tumors revealed that the fusion consistently involved the juxtaposition of *CD44* exon 1 to *SLC1A2* exon 2 (Fig. 3C and fig. S4B). Analysis of *CD44-SLC1A2* DNA sequences 3′ to the fusion junction revealed a silent C/T polymorphism in *SLC1A2* exon 4 between fusion-positive SNU16 and GC980390 (fig. S4C), confirming that the *CD44-SLC1A2* transcripts are indeed distinct entities. This apparent requirement for precise fusion may be because, among the *SLC1A2* exons, only exon 2 has a suitable alternative start ATG to initiate translation of a near-complete SLC1A2 protein. Using long-range PCR, we also confirmed the presence of *CD44/SLC1A2* genomic inversions at the DNA level in two fusion-positive clinical specimens (GC980390 and GC2000038) (Fig. 3D). No genomic inversion products were observed in the matched normal gastric samples, indicating that the *CD44/SLC1A2* inversion is a cancer-associated somatic event.

CD44-SLC1A2 silencing reduces cancer cell proliferation, invasion, and colony formation

To investigate the functional consequences of inhibiting *CD44-SLC1A2* expression, we designed a series of customized small interfering RNAs (siRNAs) targeting the *CD44-SLC1A2* fusion site. Treatment of SNU16 cells with fusion-specific siRNAs successfully silenced *CD44-SLC1A2* expression, but did not discernibly alter the independent expression of *CD44* or *SLC1A2* (Fig. 4A). Using SLC1A2 antibodies, we confirmed silencing at the protein level by both Western blotting and immunofluorescence assays (Fig. 4B and fig. S5). Similar results were obtained with a second *CD44-SLC1A2* targeting siRNA containing overlapping but distinct sequence (fig. S5). These results confirm the efficacy of the fusion-specific siRNAs.

SNU16 cells stably silenced with *CD44-SLC1A2* siRNAs resulted in a significant reduction in cell proliferation capacity compared to cells

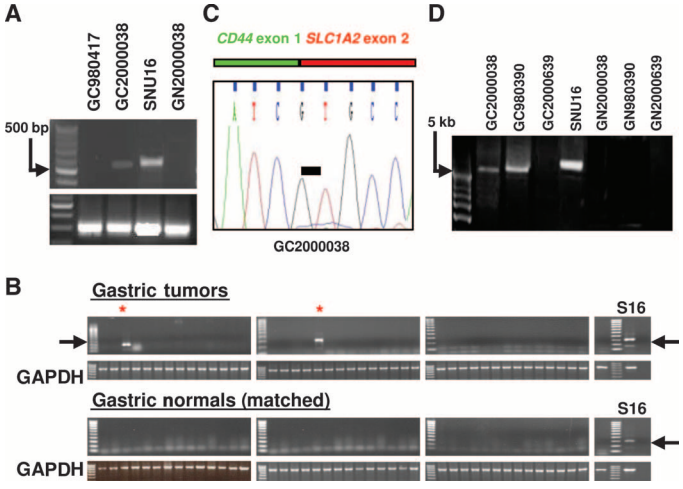

Fig. 3. *CD44-SLC1A2* expression in primary GCs. (**A**) *CD44-SLC1A2* RT-PCR on two index primary GCs (GC980417 and GC2000038) with *SLC1A2* genomic breakpoints (see Fig. 1). GN2000038 is the matched normal sample to GC2000038. Fusion-positive SNU16 cells are included as a positive control. (**B**) *CD44-SLC1A2* RT-PCR on 43 gastric tumors and matched NG tissues. Top: Tumors. Red asterisk, *CD44-SLC1A2*–expressing tumors (GC980390 and GC2000639). Bottom: Matched normal tissue. SNU16 is included as a positive control. GAPDH, glyceraldehyde-3-phosphate dehydrogenase. (**C**) Sequence of the *CD44-SLC1A2* fusion junction in GC2000038. Black bar, fusion junction. (**D**) Long-range genomic PCR analysis. Primers used are the same as in Fig. 2F. GC2000038 and GC980390 are fusion-positive primary GCs. GN2000038 and GN980390 are matched normal controls.

treated with scrambled siRNAs (Fig. 4C; $P = 0.002$, t test). No effects were observed when the fusion-specific siRNA was applied to AGS cells, which do not express *CD44-SLC1A2* (fig. S6, A and B). These results suggest that *CD44-SLC1A2* may be important for cancer cell proliferation in GC. To assess the tumorigenicity of SNU16 upon *CD44-SLC1A2* knockdown, we performed colony formation assays. Fusion-silenced cells exhibited a significantly decreased amount of anchorage-independent growth compared to controls ($P = 0.01$, Fig. 4D; see fig. S7 for enlarged figures). We then conducted Matrigel assays to investigate the effects of *CD44-SLC1A2* on cancer cell invasion. *CD44-SLC1A2*–silenced SNU16 cells also exhibited a decreased level of cell invasion compared with control cells (Fig. 4E, $P = 0.0013$), suggesting a potential role for *CD44-SLC1A2* in cell motility and invasion.

To determine whether *CD44-SLC1A2* expression might be sufficient to enhance various pro-oncogenic traits, we stably overexpressed *CD44-SLC1A2* in HFE145 NG cells. Compared to control cells, *CD44-SLC1A2*–expressing HFE145 cells exhibited enhanced cell proliferation ($P = 0.007$), colony formation ($P = 0.02$), and invasion ($P = 7.75 \times 10^{-5}$) (Fig. 4, F to H). Collectively, these results suggest that *CD44-SLC1A2* is likely required by GC cells to maintain several pro-oncogenic traits, such as proliferation, colony formation, and invasion.

The observation that *CD44-SLC1A2* produces an almost full-length SLC1A2 protein lacking only 17 amino acids raises the possibility that wild-type *SLC1A2* might also be pro-oncogenic. Indeed, silencing of wild-type SLC1A2 in AGS cells, which are fusion-negative, resulted in phenotypic effects comparable to those of *CD44-SLC1A2* silencing in SNU16 cells (fig. S8). In this regard, *CD44-SLC1A2* may be similar to oncogenic fusion genes such as *IgH-Myc* and *TMPRSS2-ERG* (*15*, *20*), where an essentially full-length pro-oncogenic protein is placed under the control of a strong transcriptional promoter.

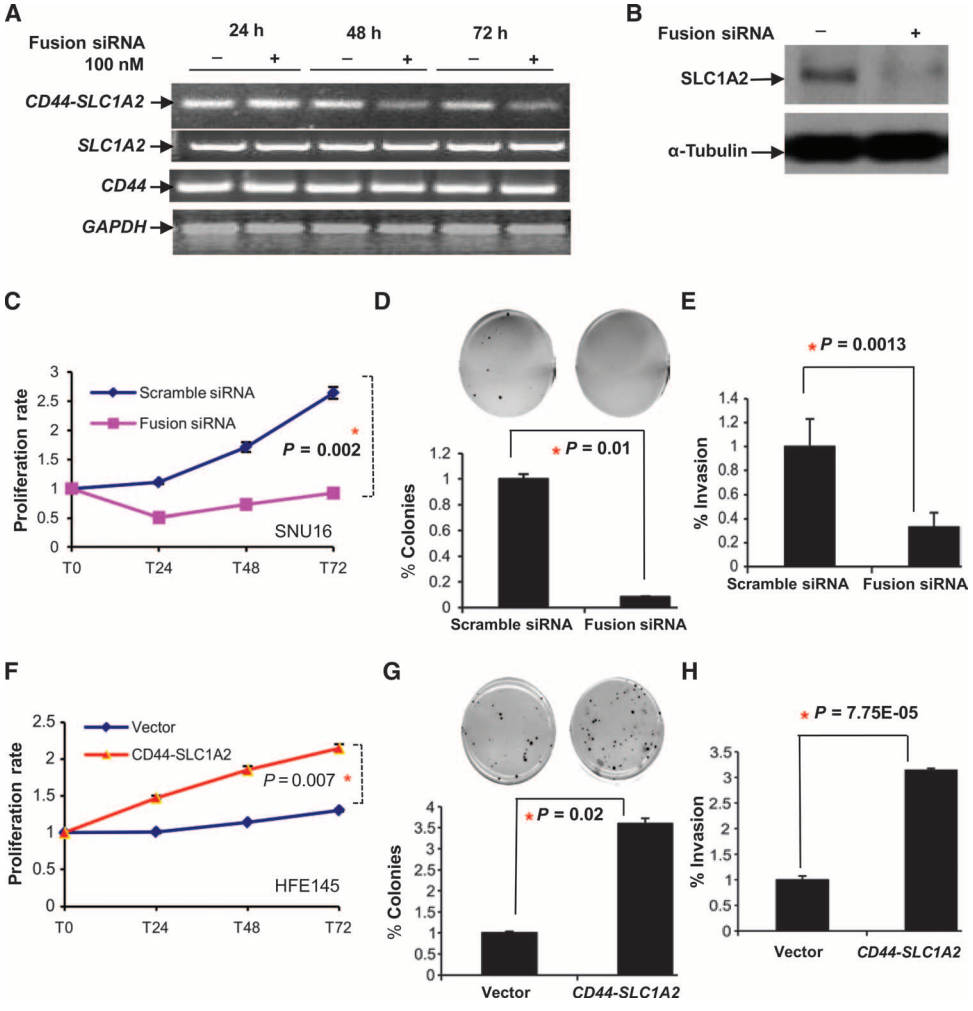

Fig. 4. *CD44-SLC1A2* fusions enhance cellular proliferation, colony formation, and invasion. (**A**) *CD44-SLC1A2* silencing by fusion-specific siRNA1 (CGCAGAUCGUGCCAACAAUUU). *CD44-SLC1A2* expression was measured 24, 48, and 72 hours after siRNA treatment. *CD44*: wild-type *CD44* expression. *CD44* primers were designed to target exons 3 to 5. *SLC1A2*: wild-type SLC1A2 expression. *SLC1A2* primers were designed to target exon 1. *GAPDH* was used as a loading control. (**B**) Western blotting. SLC1A2 protein levels were monitored with anti-SLC1A2 antibodies. α-Tubulin is used as a loading control. SNU16 cells before (–) and after (+) treatment with fusion-specific siRNAs. (**C** to **E**) Effects of *CD44-SLC1A2* knockdown. (C) Proliferation rates of SNU16 cells before and after *CD44-SLC1A2* siRNA treatment. (D) Colony formation assays with SNU16 cells before and after *CD44-SLC1A2* siRNA treatment. (E) Cell invasion assays with SNU16 cells before and after *CD44-SLC1A2* siRNA treatment. (**F** to **H**) Effects of *CD44-SLC1A2* overexpression. (F) Cell proliferation rates of HFE145 cells before and after *CD44-SLC1A2* overexpression. (G) Colony formation assays with HFE145 cells before and after *CD44-SLC1A2* overexpression. (H) Cell invasion assays with HFE145 cells before and after *CD44-SLC1A2* overexpression. All experiments were performed in triplicate. *P* values were computed with Student's *t* test. Red asterisks, *P* values exceeding the significance threshold ($P < 0.05$).

CD44-SLC1A2 silencing significantly reduces intracellular glutamate concentrations and sensitizes GC cells to chemotherapy

One possible mechanism by which *CD44-SLC1A2* may contribute to tumor development is by facilitating glutamate uptake in GC cells. In many cancers, glutamate and its related amino acid glutamine have been shown to function as important amino acids regulating tumor growth and survival (*33*, *34*). To assess the concentrations of glutamate in primary GCs, we used a colorimetric glutamate assay to measure glutamate in a panel of matched tumor and normal pairs (see Materials and Methods). Significantly elevated concentrations of glutamate were detected in primary tumors compared to matched normal stomach controls ($n = 20$; $P = 0.038$, paired t test) (Fig. 5A). To test the influence of *CD44-SLC1A2* on intracellular glutamate, we then compared concentrations of intracellular glutamate across the GC cell lines. We observed significantly higher basal glutamate concentrations in *CD44-SLC1A2*–expressing SNU16 cells than in AGS cells (Fig. 5B, $P = 0.009$). However,

after *CD44-SLC1A2* siRNA treatment, SNU16 glutamate levels were significantly reduced compared to scrambled siRNA controls (Fig. 5B, $P = 0.01$). No significant effects were observed when the fusion siRNA was applied to AGS cells (Fig. 5B). This observation suggests that *CD44-SLC1A2* may function to regulate intracellular glutamate levels in GC.

Inhibition of glutamate metabolism in cancer cells causes sensitization to pharmacologic treatment (*35*). To test whether *CD44-SLC1A2* silencing might sensitize GC cells to drug treatment, we treated control and *CD44-SLC1A2*–silenced SNU16 cells to increasing concentrations of cisplatin, a chemotherapy reagent commonly used in GC treatment, and computed GI_{50}s, the drug concentration required to cause 50% growth inhibition. We found that SNU16 cells were significantly more sensitive to cisplatin after *CD44-SLC1A2* siRNA treatment, with a reduction in GI_{50} from 11.8 to 3.96 μM ($P = 1.11 \times 10^{-6}$, Fig. 5C). The sensitization of *CD44-SLC1A2*–silenced cells appears to be specific to cisplatin, because no differences between control and silenced cells were observed upon treatment with 5-fluorouracil (5-FU), another GC chemotherapy agent (fig. S9).

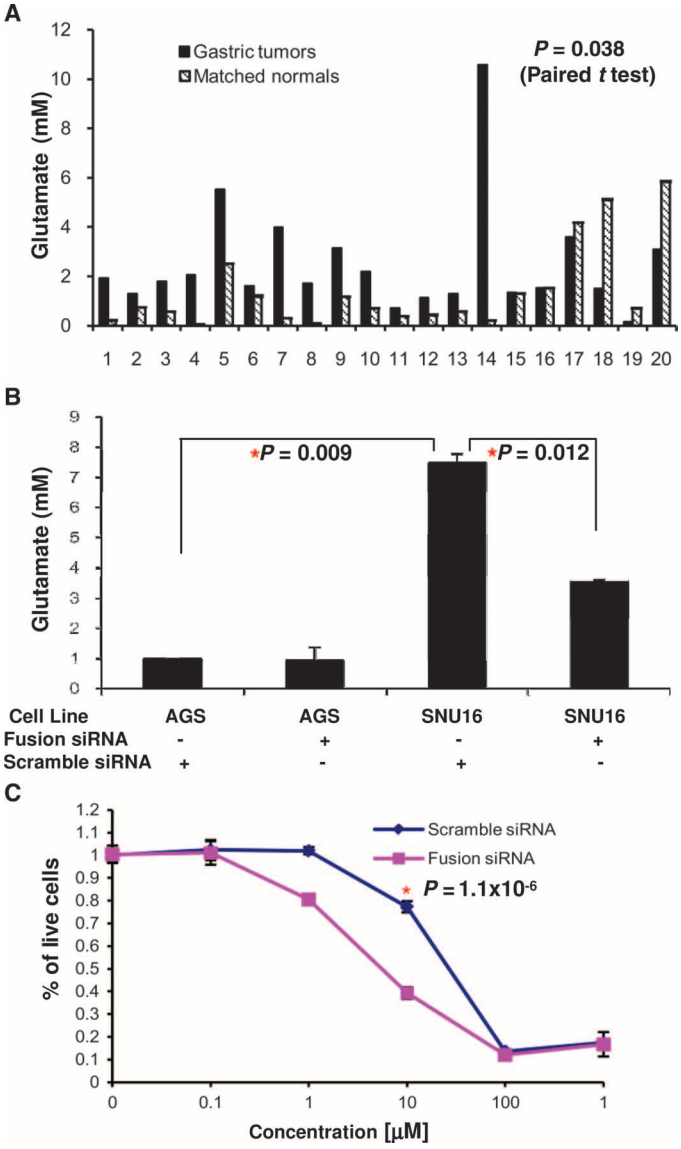

Fig. 5. *CD44-SLC1A2* regulates intracellular glutamate levels and sensitizes cells to cisplatin. (**A**) Glutamate concentrations in primary GCs compared to matched normal controls. *X* axis, 20 cancer/normal pairs. *P* values were computed with a paired *t* test comparing each tumor to its matched normal control. (**B**) Glutamate concentrations in GC cells before and after *CD44-SLC1A2* siRNA treatment. All experiments were performed in triplicate. (**C**) Cisplatin sensitivity of SNU16 cells with and without stable *CD44-SLC1A2* siRNA silencing. All experiments were performed in triplicate. *P* values were computed at 10 μM cisplatin. *P* values for (B) and (C) were computed with a *t* test. Red asterisk, *P* values exceeding the significance threshold ($P < 0.05$).

Tumors expressing high *SLC1A2* levels are associated with *CD44-SLC1A2* positivity

CD44 is highly expressed in many cancers including GC (*36*). One consequence of the *CD44-SLC1A2* fusion might thus be to place *SLC1A2* under the regulatory control of *CD44* promoter elements, causing high amounts of *SLC1A2* expression in tumors. If this were true, tumors expressing high *SLC1A2* levels should also tend to be *CD44-SLC1A2*–positive. To explore this possibility, we queried a previously described gene expression database of 197 GCs to identify tumors expressing high *SLC1A2* levels (*37*). We screened 15 GCs from the top 15% of *SLC1A2*-overexpressing tumors for *CD44-SLC1A2* expression. Among the 15 tumors, five GCs expressed the *CD44-SLC1A2* fusion transcript (Fig. 6, blue crosses), and none of the matched adjacent normal tissues expressed *CD44-SLC1A2* (Fig. 6). Thus, whereas the rate of *CD44-SLC1A2* positivity in an unselected patient cohort is low (1 to 2%), the *CD44-SLC1A2* positivity rate is elevated in this selected subpopulation (33%, 5 of 15 tumors). This result is consistent with the *CD44-SLC1A2* fusion causing the transcriptional up-regulation of *SLC1A2*. In *CD44-SLC1A2*–negative tumors, high *SLC1A2* levels may be due to alternative mechanisms, such as focal genomic amplification, fusion to other partners, and epidermal growth factor (EGF) or mammalian target of rapamycin (mTOR)/Akt signaling (*38*, *39*).

An unsupervised clustering analysis of the 197 gastric tumor gene expression profiles revealed that most of high *SLC1A2*–expressing tumors tended to cluster together (>75%), suggesting that high *SLC1A2* expression

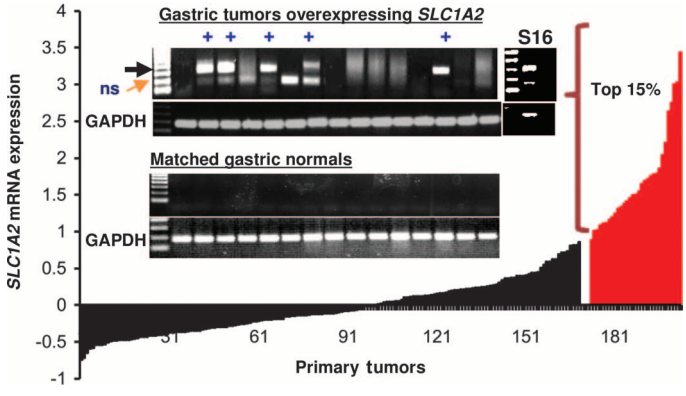

Fig. 6. *CD44-SLC1A2*–positive tumors are associated with high *SLC1A2* expression. Graph: *SLC1A2* mRNA expression in 197 GCs. Gene expression data were median-centered. The top 15% of high *SLC1A2*–expressing tumors are shown in red. Inset: RT-PCR screening of *CD44-SLC1A2* in the top 15% of high *SLC1A2*–expressing GCs and matching 15 NG tissues. *GAPDH* was used as a loading control. Blue crosses, samples expressing CD44-SLC1A2. SNU16 cells (S16) were included as a positive control. The smaller band of 200 bp was sequenced and identified to be nonspecific (ns).

may define a distinct molecular subgroup of GC (fig. S10). To identify predominant biological themes associated with this molecular subgroup, we performed gene ontology (GO) analysis on a 710-gene "*SLC1A2* signature," generated by comparing the top 15% of high *SLC1A2*–expressing tumors against the bottom 15% [Wilcoxon signed rank test, false discovery rate (FDR) = 0.005]. Genes expressed in high *SLC1A2*–expressing tumors were associated with ribosomal biosynthesis and protein translation (corrected $P = 5.12 \times 10^{-33}$, Fisher's test; table S2). These results suggest that tumors expressing high *SLC1A2* levels, by either *CD44* fusion or alternative mechanisms, may comprise a distinct subclass of GC.

CD44-SLC1A2 expression can occur independently of 11p13 amplification

Although *CD44-SLC1A2* was initially identified in tumors exhibiting 11p13 amplification (Fig. 1B), 11p13 amplification may not be an absolute prerequisite for *CD44-SLC1A2* fusion expression. To investigate the relationship between 11p13 genomic amplification and *CD44-SLC1A2* expression, we analyzed seven fusion-positive tumors using Affymetrix SNP6 arrays. Of seven fusion-positive tumors, two tumors (GC980390 and GC990172) exhibited evidence of 11p13 genomic amplification, whereas the other five did not (fig. S11). This finding demonstrates that *CD44-SLC1A2* expression can be observed in tumors independent of 11p13 genomic amplification. To further investigate the notion that 11p13 amplification and *CD44-SLC1A2* gene fusion are distinct events, we compared *CD44* and *SLC1A2* expression across 45 gastric tumors, including (i) 11p13-nonamplified samples (32 samples), (ii) 11p13-amplified but fusion-negative samples (6 samples), and (iii) *CD44-SLC1A2* fusion-positive samples (7 samples). The rate of 11p13 amplification in this series (~17%) is similar to frequencies previously reported in the literature (*40*). It is important to note that in this experiment, the expression measurements were inferred using U133P2 Affymetrix microarray probes, which target the 3′ ends of genes. Compared to nonamplified samples, fusion-positive samples exhibited significantly increased 3′ *SLC1A2* gene expression ($P = 0.004$), but 11p13-amplified samples did not ($P = 0.86$) (fig. S11A). These findings suggest that high *SLC1A2* expression levels may be driven more by fusion events rather than by generalized 11p13 amplification. The one exception was a sample with a high-level focal 11p13 amplification (GC980417); in this tumor, *SLC1A2* was highly expressed (fig. S11A). Intriguingly, unlike *SLC1A2*, a very different scenario was observed for *CD44*. Specifically, although *CD44* 3′ transcripts were significantly overexpressed in 11p13-amplified tumors ($P = 0.016$), they were significantly underexpressed in fusion-positive tumors ($P = 0.006$) (fig. S11B). We speculate that this latter finding may be due to the *CD44/SLC1A2* genomic inversion decoupling the 3′ end of the *CD44* gene (the region detected by the Affymetrix array) from the endogenous *CD44* promoter. Additional evidence of this decoupling was obtained in a real-time PCR analysis measuring *SLC1A2* exon 1, where, unlike the 3′ *SLC1A2* transcripts, *SLC1A2* exon 1 (which is not part of the *CD44-SLC1A2* fusion) was not observed to be highly expressed relative to nonamplified samples in fusion-positive samples (fig. S11, C and D).

DISCUSSION

The cancer-specific nature of fusion genes has earned them an important place in many translational cancer research applications, including molecular subtyping, monitoring for disease relapse, and as drug targets. In pediatric acute lymphoblastic leukemia (ALL), expression of *AML-ETO* and *PML-RAR* is routinely used to diagnose particular clinical subtypes (*17*), and treatment of CML has been revolutionized by imatinib, an inhibitor of the *BCR-ABL* fusion gene (*18*). Along with *AGTRAP-BRAF* fusions (*22*), *CD44-SLC1A2* represents another recurrent gene fusion identified in a major GI cancer, providing further evidence for the existence of this important class of molecular aberrations in GI malignancies.

Here, we used GBA to uncover the existence of *CD44-SLC1A2* gene fusions in GC. Notably, although GBA has been previously used for fusion gene discovery in leukemia (*27*, *41*), our study demonstrates that this approach can also highlight potential fusion genes in solid epithelial tumors. Among genes exhibiting genomic breakpoints, we prioritized genes for study based on their rate of recurrence in multiple samples and occurrence in a cell line to serve as an experimental model. Using these two criteria, we nominated only two genes: *SLC1A2* and *ZNF1A3*. We note that GBA does come with a few caveats, because fusion events arising from balanced chromosomal rearrangements would not alter overall copy number levels and are unlikely to be detected. However, GBA has the advantage of being readily applicable to aCGH data, for which there are already numerous large-scale data sets readily available in the public domain (*42*). Revisiting these data sets may identify additional genes recurrently targeted by genomic breakpoints in solid cancers.

The identification of *SLC1A2*, a glutamate transporter, as a fusion gene participant is notable. To date, the vast majority of known oncogenic fusion events have largely involved transcription factors (for example, *Myc* and *RAR*) or kinases (for example, *BCR-ABL*) (*15*–*17*). The discovery of *CD44-SLC1A2* raises the intriguing possibility that oncogenic gene fusions may also target genes involved in cancer metabolism. Specifically, the *CD44-SLC1A2* gene fusion is predicted to produce a slightly truncated *SLC1A2* protein that retains most of the key protein domains required for glutamate transporter fusion, and may function to facilitate glutamate accumulation in GC cells. A substantial body of evidence has implicated glutamate and glutamine as critical amino acids necessary for the maintenance and elaboration of cancer-specific traits (*43*). For example, glutamate and glutamine have been shown to regulate tumor growth and oncogenic signals such as mTOR (*44*). The requirement of cancer cells for glutamate may also be related to the Warburg effect, a universal feature of cancer cells where they exhibit overactive glycolysis because of a deficiency in channeling glycolytic metabolites into the tricarboxylic acid (TCA) cycle for adenosine triphosphate (ATP) generation. Glutamate may provide cancer cells with an alternative route of ATP production because intracellular glutamate and glutamine can also be converted into α-ketoglutarate, a TCA cycle intermediate (*45*). Glutamate levels have been shown to be elevated in many cancers, and in our study, we confirmed that glutamate levels are also elevated in gastric tumors compared to normal stomach, consistent with a previous report (*46*).

The absolute rate of *CD44-SLC1A2* positivity was relatively low in this study (1 to 2%); however, analyses of larger GC patient cohorts will be required to determine the true *CD44-SLC1A2* positivity rate. Nevertheless, we note that even low-frequency events in cancer can prove therapeutically useful, as shown by *EML4-ALK* fusions in lung cancer (1 to 5%) (*21*) and *RAF* fusions in gastric, melanoma, and prostate cancers (*22*). As a cell membrane–bound receptor, *CD44-SLC1A2* may prove amenable to targeting using either small molecules or therapeutic antibodies. Several of the *CD44-SLC1A2*–positive GCs in our study also

exhibited focal amplifications in genes specifically related to RTK (receptor tyrosine kinase)/RAS/MAPK (mitogen-activated protein kinase) signaling, including SNU16 (*FGFR2*), GC2000114 (*MET*), GC2000639 (*KRAS*), and GC980390 (*ERBB2*). *CD44-SLC1A2* may collaborate with these canonical oncogenes to facilitate MAPK signaling in GC. Beyond its effects in cancer development, targeting *CD44-SLC1A2* in fusion-positive tumors may also represent a promising avenue for sensitizing GCs to commonly used standard-of-care chemotherapies, because silencing *CD44-SLC1A2* was sufficient to cause a significant sensitization of GC cells to cisplatin in vitro. It will be interesting to evaluate the potential of *CD44-SLC1A2* as a potential drug target, and determining exactly how this gene fusion, and possibly other glutamate-related transporters, might contribute to GC development by establishing a metabolic environment favoring oncogenesis.

MATERIALS AND METHODS

Primary tumors and cell lines

Primary gastric tumors were obtained from the SingHealth Tissue Repository, an institutional resource of National Cancer Centre of Singapore and Singapore General Hospital. All patient samples were obtained with informed patient consent and approvals from Institutional Review Boards and Ethics Committees. GC cell lines AGS, KATO III, SNU1, SNU16, N87, and Hs746T were purchased from the American Type Culture Collection. AZ521, Ist1, TMK1, MKN1, MKN7, MKN28, MKN45, MKN74, Fu97, and IM95 cells were obtained from the Japan Health Science Research Resource Bank. SCH cells were provided by Y. Ito (Cancer Sciences Institute of Singapore). YCC cells were a gift from S.-Y. Rha (Yonsei Cancer Center, South Korea).

RNA and DNA extraction

Genomic DNA from samples was extracted with a Qiagen Blood and Cell Culture DNA extraction kit. Total RNA was extracted with RNA extraction reagents (Qiagen). Both RNAs and DNAs were quantitated with either NanoDrop ND-1000 (NanoDrop Technologies) or Agilent Bioanalyzer 2100 (Agilent Technologies).

GBA

GBA was performed on a panel of 106 primary tumors and 27 cell lines with Agilent 244K Human Genome Microarrays (Agilent Technologies). Sample labeling and hybridizations were performed according to the manufacturer's instructions. Tumor and control genomic DNAs (human spleen DNA) were labeled with Cy3-dUTP (deoxyuridine triphosphate) and Cy5-dUTP, respectively. Hybridized slides were scanned on an Agilent DNA Microarray Scanner (Agilent Technologies), and images were extracted with Agilent Feature Extraction software. Data were analyzed with Agilent CGH Analytics software (v.3.5) using a *Z*-score algorithm with a threshold of 2.0 and a one-point window to identify genomic breakpoints.

FISH

SNU16 interphase and metaphase cell pellets were prepared for FISH analysis by standard hypotonic treatment and fixation after colcemid exposure (10 μg/ml) for 2 hours. Before hybridization, cells were pretreated with pepsin (100 mg/ml) (Sigma) and 0.01 M HCl at 37°C (5 min), fixed in 1% formaldehyde (Sigma) (10 min), and dehydrated in an ethanol series. Fosmid and bacterial artificial chromosome (BAC) probes were obtained from BACPAC Resource Center (CHORI) and grown following vendor instructions. DNA was extracted with Nucleobond PC500 (Macherey-Nagel), followed by labeling with either biotin-16–dUTP (Roche) or digoxigenin-11–dUTP (Roche) with an Enzo Nick Translation DNA labeling system. About 20 ng of each probe was used per hybridization in addition to 10 μg of Cot-1 DNA (Invitrogen). The slide and probe mixes were co-denatured on a hot plate set at 75°C and hybridized overnight at 37°C. Posthybridization washes were performed at 45°C in 50% prewarmed formamide/2× SSC solution (twice), followed by two washes in 2× SSC (twice). Slides were blocked with blocking reagent (Roche), followed by incubation with avidin-conjugated fluorescein isothiocyanate (FITC) (Roche) and anti–digoxigenin-rhodamine (Roche), respectively. 4′,6-Diamidino-2-phenylindole (DAPI) counterstain (Vector Laboratories) was then used to stain the nuclei to enable visualization. Slides were mounted with Vectashield (Vector Laboratories). Fluorescence images were captured with a 60× objective using a cooled charge-coupled device (CCD) camera attached to a Nikon fluorescence microscope. Automated image capture was performed with ISIS software (Metasystems).

RLM-RACE

5′ RACE. RLM-RACE was performed with the FirstChoice RLM-RACE kit (Applied Biosystems). Total RNA (10 μg) was first treated with calf intestinal alkaline phosphatase (CIP) to remove 5′ phosphate groups, followed by tobacco acid pyrophosphatase to remove 5′ cap structures. After RNA linker ligation, mRNA transcripts were reverse-transcribed with Moloney murine leukemia virus (MMLV) reverse transcriptase. To amplify first-strand cDNAs, we performed outer 5′ PCR using 5′ RACE outer primers and a *SLC1A2* exon 3 primer (ACACACTGCTCCCAGGATGA) with SuperTaq Plus polymerase (Applied Biosystems). Subsequently, inner 5′ PCR was performed with a 5′ RACE inner primer (provided in kit) and a *SLC1A2* exon 2 primer (AGCCAAGATGACTGTCGTGCATTC). After gel electrophoresis, PCR bands of interest were excised and cloned into pCR 4-TOPO (Invitrogen) vectors. Purified plasmid DNAs were sequenced bidirectionally on an ABI 3730 automated sequencer (Applied Biosystems). A minimum of five independent colonies were sequenced in each experiment.

3′ RACE. RLM-RACE was performed with the FirstChoice RLM-RACE kit (Applied Biosystems). Total RNA (1 μg) was reverse-transcribed with a 3′ RACE adaptor and reverse transcriptase provided in the kit. To amplify first-strand cDNAs, we performed outer 3′ PCR using 3′ RACE outer primers and a *SLC1A2* exon 1 primer (TTGAGGCGCTAAAGGGCTTACC) with SuperTaq Plus polymerase (Applied Biosystems). Subsequently, inner 3′ PCR was performed with a 3′ RACE inner primer (provided in kit) and a separate *SLC1A2* exon 1 primer (CAGACCATGGCATCTACGGAAGG). After gel electrophoresis, PCR bands of interest were excised and cloned into PCR 4-TOPO (Invitrogen) vectors. Purified plasmid DNAs were sequenced bidirectionally on an ABI 3730 automated sequencer (Applied Biosystems). A minimum of five independent colonies were sequenced in each experiment.

Semiquantitative and quantitative RT-PCR

Semiquantitative RT-PCR. GC RNAs were reverse-transcribed by SuperScript II reverse transcriptase enzyme with oligo-dT (T18) primers (Invitrogen). To detect *CD44-SLC1A2*, we performed RT-PCR using forward primers to *CD44* exon 1 (CCATGGACAAGT-

TTTGGTGGCA) and reverse primers to *SLC1A2* exon 3 (GTATATCCCCTGGGAAGGCT), exon 4 (CAGCTGCTTCTTGAGCTTGGGA), exon 5 (AAGCAGGCTTGGACAAGGTT), or exon 6 (CTCGTTCAACAGAGAGACAACAGC). Products were resolved by gel electrophoresis, and bands of interest were excised and cloned for subsequent analysis. To evaluate wild-type *CD44* and *SLC1A2* expression independently of *CD44-SLC1A2*, we used *CD44* primers targeting exons 3 to 5, and *SLC1A2* primers targeting exon 1. *CD44-SLC1A2* RT-PCR involving clinical specimens (Fig. 3) was performed in an unselected cohort of GC patients. Reactions were repeated a minimum of three independent times.

Quantitative RT-PCR. SNU16 GC cells lines and nine primary gastric tumors were selected for quantitative RT-PCR (qRT-PCR) analysis. T1, T2, and T3 were group 1 gastric tumors that are 11p13 amplification–negative and fusion-negative; T4, T5, and T6 are group 2 tumors that are 11p13-amplified but do not express *CD44-SLC1A2*; T7, T8, and T9 were group 3 tumors expressing *CD44-SLC1A2* but are 11p13-nonamplified. Briefly, 2 μg of RNA was reverse-transcribed by SuperScript III reverse transcriptase enzyme with oligo-dT (T18) primers (Invitrogen). qRT-PCR was performed with QuantiFast SYBR Green PCR kit (Qiagen) following the manufacturer's instructions. Primers used were the following: fusion forward primer targeting *CD44* exon 1 (TTCGGTCCGCCATCCTCGTC) and reverse primer targeting *SLC1A2* exon 2 (CACTTCCACCTGCTTGGGCA); *SLC1A2* exon 1 forward primer (GCCCGTTGAGGCGCTAAAGG) and reverse primer (AGCACTATCCGGCAGCTGTG); and *GAPDH* forward primer (CCACCCAGAAGACTGTGGATGG) and reverse primer (CACTGACACGTTGGCAGTGG). Samples were analyzed with Applied Biosystems 7900HT system.

DNA sequencing

Purified PCR products were sequenced in forward and reverse directions with the ABI PRISM BigDye Terminator Cycle Sequencing Ready Reaction kit (version 3) and ABI PRISM 3730 Genetic Analyzer (Applied Biosystems). Chromatograms were analyzed by SeqScape V2.5 and manual review.

Fiber-FISH

SNU16 cells and control cells (normal lymphoblastoid CCL159) were grown in RPMI 1640 enriched with 15% fetal bovine serum (FBS), 1% penicillin-streptomycin, and 1% L-glutamine. Each cell suspension (2 to 3 ml) was centrifuged at 1200 rpm for 12 min and then washed with 6 ml of phosphate-buffered saline (PBS) twice. Pellets were diluted with PBS to a final concentration of about 2×10^4 to 3×10^4/ml. Each cell suspension (10 μl) was spread on a poly-L-lysine (Sigma)–coated slide, air-dried, and then fitted into a Cadenza coverslip according to the manufacturer's recommendations (Thermo Shandon). Freshly made lysis solution (150 μl) (5:2 70 mM NaOH/absolute ethanol) was applied to the slides, followed by 150 μl of 96% ethanol. Slides were air-dried at room temperature, treated with 3:1 acetic acid/ethanol fixative for 5 min, and dehydrated in ethanol series (70, 90, and 100%) for 3 min each. The FISH procedure was then applied.

Long-range genomic PCR

CD44/SLC1A2 chromosomal inversions were detected with a long-range PCR kit (Qiagen) following the manufacturer's instructions. Reactions were performed with a forward primer at *CD44* exon 1 (GAAGAAAGCCAGTGCGTCTC, positive strand) and a reverse primer at *SLC1A2* intron 1 in the minimal breakpoint region (GAGGGCTGTCCTTAACGCCTAGC, negative strand). Experiments were repeated a minimum of three independent times.

Western blotting

Cells were harvested in lysis buffer [10 mM tris-Cl (pH 7.5), 150 mM NaCl, 1% Triton X-114] for 1 hour at 4°C and centrifuged at 800*g*. Supernatants were incubated at 30°C for 5 to 10 min and further centrifuged at 300*g* at room temperature. Western blotting was performed on membrane fractions with the following antibodies and dilutions: SLC1A2/EAAT2 (1:500; Cell Signaling Technology) and α-tubulin (1:2000; Cell Signaling Technology). Experiments were repeated a minimum of three independent times.

Immunofluorescence staining

Cells were fixed with 3.7% formaldehyde followed by permeabilization with 0.1% Triton X-100. After three washes with 1× PBS, cells were blocked with 1% bovine serum albumin (BSA). Subsequently, cells were incubated with primary *SLC1A2* antibodies (Cell Signaling Technology) for 2 hours followed by 2-hour secondary antibody (Sigma) incubation. Images were taken with a Nikon Eclipse TE2000-U microscope.

CD44-SLC1A2 siRNA transfections and overexpression

GC cells were transfected with either specific siRNAs targeted to the *CD44-SLC1A2* fusion site (100 nM, custom siRNA siGENOME with SMART selection, Dharmacon) or negative control scrambled siRNAs with siPORT *NeoFX* transfection reagent (Applied Biosystems) in Opti-MEM (Invitrogen) following the manufacturer's protocol. After 24, 48, and 72 hours of siRNA treatment, cells were subjected for downstream analysis. For wild-type *SLC1A2* siRNAs, GC cells were transfected with specific nonoverlapping siRNAs targeted to either *SLC1A2* exon 1 or *SLC1A2* downstream regions (100 nM, custom siRNA siGENOME with SMART selection, Dharmacon) or negative control scrambled siRNAs with siPORT *NeoFX* transfection reagent (Applied Biosystems) in Opti-MEM (Invitrogen) following the manufacturer's protocol. For overexpression studies, the full-length coding regions of *CD44-SLC1A2* cDNA were inserted into the pEGFP-N1 vector. Control vectors or fusion green fluorescent protein (GFP) vectors were introduced into HFE145 cells, and stable transfectants were selected with G418 (stable overexpression) or puromycin (stable knockdown) for 4 weeks.

Cell proliferation assay and invasion assays

Cell proliferation assays were performed with a CellTiter96 Aqueous Nonradioactive Cell Proliferation Assay kit (Promega) following the manufacturer's instructions, and the plates were measured with a Perkin-Elmer plate reader. Cell invasion assays were performed with Biocoat Matrigel invasion chambers with 8-μm pore filter inserts (BD Biosciences). Forty-eight hours after transfection, 5×10^4 cells were transferred to the upper Matrigel chamber in 500 μl of serum-free medium and incubated for 24 hours. Invading cells were counted with light microscopy. Each assay was performed in triplicate, and the results were averaged over three independent experiments.

Colony formation assays

Base layers of 0.5% gum agar in 1× McCoy's 5A and 10% FBS were poured into six-well plates and allowed to harden at 4°C. After 48 hours of siRNA transfection, 50,000 cells per well were seeded in complete

medium plus agar mixture at 42°C and seeded on top of the solidified base layer. Plates were incubated at 37°C for 3 to 4 weeks, during which plates were fed dropwise with complete medium. After 3 to 4 weeks, plates were photographed with the Kodak GL 200 System (EpiWhite illumination). Each assay was performed in triplicate, and the results were averaged over three independent experiments.

Glutamate assays and drug treatments

GC cells and primary tissues were lysed in glutamate assay buffer, and glutamate concentrations were determined with a Glutamate Assay Kit (BioVision). Briefly, to each cellular lysate, a vendor-provided glutamate enzyme mix was added, which recognizes glutamate as a specific substrate, leading to proportional color development. For cisplatin treatments, cells were seeded into 96-well plates after siRNA transfection. Subsequently, cisplatin or 5-FU at increasing dosages (0 to 1 mM) was added to respective wells. Cells were subjected to MTS [3-(4,5-dimethylthiazol-2-yl)-5-(3-carboxymethoxyphenyl)-2-(4-sulfophenyl)-2*H*-tetrazolium] proliferation assays after 48 hours of drug treatment. Each assay was performed in triplicate, and the results were averaged over three independent experiments.

Copy number analysis (Affymetrix)

Affymetrix SNP6 arrays were processed with Affymetrix GTC 4.0 software, and tumor profiles were normalized against a matched normal reference. The data were visualized with Nexus 5.0 software (Biodiscovery). A rank segmentation algorithm, a variation of the segmentation method based on circular binary segmentation, was used to segment the copy number data across the genome.

Gene expression analysis

Gene expression data are available from the Gene Expression Omnibus database under accession number GSE15460. Gene expression profiles (Affymetrix U133P2 arrays) were normalized with the MAS5 algorithm. Comparisons between *CD44* and *SLC1A2* expression values were performed on a subset of 45 samples for which gene expression, copy number information, and *CD44-SLC1A2* gene fusion status were available. Unsupervised clustering was based on all probe sets after removing the bottom 25% of probes with the lowest interquantile range. Hierarchical clustering and Wilcoxon signed rank tests were performed with R software 2.9.0. FDR q-value calculations were calculated with the R package "qvalue." GO analysis was performed with the DAVID database.

Statistical analysis

Experiments were assessed by Student's unpaired t test, with the exception of the tumor/normal glutamate measurements, where a paired t test was used. P values of <0.05 were considered statistically significant.

SUPPLEMENTARY MATERIAL

www.sciencetranslationalmedicine.org/cgi/content/full/3/77/77ra30/DC1

Fig. S1. *MYC*, *ERBB2*, *RAB23*, and *PTEN* genomic aberrations in SNU16, N87, HS746T, and TMK1 cells detected by aCGH.

Fig. S2. 3′ RACE and full-length *CD44-SLC1A2* expression in SNU16 cells.

Fig. S3. Chromosomal inversion model of *CD44-SLC1A2* gene fusion.

Fig. S4. Predicted protein structure of *CD44-SLC1A2* and expression in primary GCs.

Fig. S5. Silencing *CD44-SLC1A2* with a second fusion-specific siRNA inhibits cellular proliferation, invasion, and colony formation.

Fig. S6. *CD44-SLC1A2* silencing does not affect AGS cells.

Fig. S7. Soft agar assays with two fusion-specific siRNAs.

Fig. S8. Reduction of cellular proliferation in fusion-negative AGS cells after silencing of wild-type *SLC1A2*.

Fig. S9. *CD44-SLC1A2* knockdown does not sensitize cells to 5-fluorouracil chemotherapy.

Fig. S10. Unsupervised clustering of GC expression profiles reveals clustering of high *SLC1A2*–expressing tumors.

Fig. S11. 11p13 copy number status in CD44-SLC1A2–expressing samples.

Fig. S12. *CD44* and *SLC1A2* expression levels of 11p13-nonamplified, 11p13-amplified, and fusion-positive samples.

Table S1. Gene exhibiting genomic breakpoints.

Table S2. Gene ontology analysis of high SLC1A2–expressing tumors.

References

REFERENCES AND NOTES

1. H. Brenner, D. Rothenbacher, V. Arndt, Epidemiology of stomach cancer. *Methods Mol. Biol.* **472**, 467–477 (2009).
2. H. H. Hartgrink, E. P. Jansen, N. C. van Grieken, C. J. van de Velde, Gastric cancer. *Lancet* **374**, 477–490 (2009).
3. F. Kamangar, G. M. Dores, W. F. Anderson, Patterns of cancer incidence, mortality, and prevalence across five continents: Defining priorities to reduce cancer disparities in different geographic regions of the world. *J. Clin. Oncol.* **24**, 2137–2150 (2006).
4. W. C. Lee, Breast, stomach and colorectal cancer screening in Korea. *J. Med. Screen.* **13** (Suppl. 1), S20–S22 (2006).
5. C. Hamashima, D. Shibuya, H. Yamazaki, K. Inoue, A. Fukao, H. Saito, T. Sobue, The Japanese guidelines for gastric cancer screening. *Jpn. J. Clin. Oncol.* **38**, 259–267 (2008).
6. C. Jackson, D. Cunningham, J. Oliveira; ESMO Guidelines Working Group, Gastric cancer: ESMO clinical recommendations for diagnosis, treatment and follow-up. *Ann. Oncol.* **20** (Suppl. 4), 34–36 (2009).
7. E. M. El-Omar, M. Carrington, W. H. Chow, K. E. McColl, J. H. Bream, H. A. Young, J. Herrera, J. Lissowska, C. C. Yuan, N. Rothman, G. Lanyon, M. Martin, J. F. Fraumeni Jr., C. S. Rabkin, Interleukin-1 polymorphisms associated with increased risk of gastric cancer. *Nature* **404**, 398–402 (2000).
8. G. L. Hold, C. S. Rabkin, W. H. Chow, M. G. Smith, M. D. Gammon, H. A. Risch, T. L. Vaughan, K. E. McColl, J. Lissowska, W. Zatonski, J. B. Schoenberg, W. J. Blot, N. A. Mowat, J. F. Fraumeni Jr., E. M. El-Omar, A functional polymorphism of toll-like receptor 4 gene increases risk of gastric carcinoma and its precursors. *Gastroenterology* **132**, 905–912 (2007).
9. P. Guilford, J. Hopkins, J. Harraway, M. McLeod, N. McLeod, P. Harawira, H. Taite, R. Scoular, A. Miller, A. E. Reeve, E-cadherin germline mutations in familial gastric cancer. *Nature* **392**, 402–405 (1998).
10. G. Tamura, T. Kihana, K. Nomura, M. Terada, T. Sugimura, S. Hirohashi, Detection of frequent *p53* gene mutations in primary gastric cancer by cell sorting and polymerase chain reaction single-strand conformation polymorphism analysis. *Cancer Res.* **51**, 3056–3058 (1991).
11. Q. L. Li, K. Ito, C. Sakakura, H. Fukamachi, K. Inoue, X. Z. Chi, K. Y. Lee, S. Nomura, C. W. Lee, S. B. Han, H. M. Kim, W. J. Kim, H. Yamamoto, N. Yamashita, T. Yano, T. Ikeda, S. Itohara, J. Inazawa, T. Abe, A. Hagiwara, H. Yamagishi, A. Ooe, A. Kaneda, T. Sugimura, T. Ushijima, S. C. Bae, Y. Ito, Causal relationship between the loss of *RUNX3* expression and gastric cancer. *Cell* **109**, 113–124 (2002).
12. K. F. Pan, W. G. Liu, L. Zhang, W. C. You, Y. Y. Lu, Mutations in components of the Wnt signaling pathway in gastric cancer. *World J. Gastroenterol.* **14**, 1570–1574 (2008).
13. S. T. Tay, S. H. Leong, K. Yu, A. Aggarwal, S. Y. Tan, C. H. Lee, K. Wong, J. Visvanathan, D. Lim, W. K. Wong, K. C. Soo, O. L. Kon, P. Tan, A combined comparative genomic hybridization and expression microarray analysis of gastric cancer reveals novel molecular subtypes. *Cancer Res.* **63**, 3309–3316 (2003).
14. F. Mitelman, B. Johansson, F. Mertens, The impact of translocations and gene fusions on cancer causation. *Nat. Rev. Cancer* **7**, 233–245 (2007).
15. T. H. Rabbitts, T. Boehm, Structural and functional chimerism results from chromosomal translocation in lymphoid tumors. *Adv. Immunol.* **50**, 119–146 (1991).
16. A. de Klein, A. G. van Kessel, G. Grosveld, C. R. Bartram, A. Hagemeijer, D. Bootsma, N. K. Spurr, N. Heisterkamp, J. Groffen, J. R. Stephenson, A cellular oncogene is translocated to the Philadelphia chromosome in chronic myelocytic leukaemia. *Nature* **300**, 765–767 (1982).
17. S. H. Ghaffari, S. Rostami, D. Bashash, K. Alimoghaddam, A. Ghavamzadeh, Real-time PCR analysis of PML-RARα in newly diagnosed acute promyelocytic leukaemia patients treated with arsenic trioxide as a front-line therapy. *Ann. Oncol.* **17**, 1553–1559 (2006).
18. M. Deininger, E. Buchdunger, B. J. Druker, The development of imatinib as a therapeutic agent for chronic myeloid leukemia. *Blood* **105**, 2640–2653 (2005).
19. S. Heim, F. Mitelman, Molecular screening for new fusion genes in cancer. *Nat. Genet.* **40**, 685–686 (2008).

20. S. A. Tomlins, D. R. Rhodes, S. Perner, S. M. Dhanasekaran, R. Mehra, X. W. Sun, S. Varambally, X. Cao, J. Tchinda, R. Kuefer, C. Lee, J. E. Montie, R. B. Shah, K. J. Pienta, M. A. Rubin, A. M. Chinnaiyan, Recurrent fusion of *TMPRSS2* and ETS transcription factor genes in prostate cancer. *Science* **310**, 644–648 (2005).
21. M. Soda, Y. L. Choi, M. Enomoto, S. Takada, Y. Yamashita, S. Ishikawa, S. Fujiwara, H. Watanabe, K. Kurashina, H. Hatanaka, M. Bando, S. Ohno, Y. Ishikawa, H. Aburatani, T. Niki, Y. Sohara, Y. Sugiyama, H. Mano, Identification of the transforming *EML4–ALK* fusion gene in non-small-cell lung cancer. *Nature* **448**, 561–566 (2007).
22. N. Palanisamy, B. Ateeq, S. Kalyana-Sundaram, D. Pflueger, K. Ramnarayanan, S. Shankar, B. Han, Q. Cao, X. Cao, K. Suleman, C. Kumar-Sinha, S. M. Dhanasekaran, Y. B. Chen, R. Esgueva, S. Banerjee, C. J. LaFargue, J. Siddiqui, F. Demichelis, P. Moeller, T. A. Bismar, R. Kuefer, D. R. Fullen, T. M. Johnson, J. K. Greenson, T. J. Giordano, P. Tan, S. A. Tomlins, S. Varambally, M. A. Rubin, C. A. Maher, A. M. Chinnaiyan, Rearrangements of the *RAF* kinase pathway in prostate cancer, gastric cancer and melanoma. *Nat. Med.* **16**, 793–798 (2010).
23. F. Mitsui, Y. Dobashi, I. Imoto, J. Inazawa, K. Kono, H. Fujii, A. Ooi, Non-incidental coamplification of *Myc* and *ERBB2*, and *Myc* and *EGFR*, in gastric adenocarcinomas. *Mod. Pathol.* **20**, 622–631 (2007).
24. A. Varis, M. Wolf, O. Monni, M. L. Vakkari, A. Kokkola, C. Moskaluk, H. Frierson Jr., S. M. Powell, S. Knuutila, A. Kallioniemi, W. El-Rifai, Targets of gene amplification and overexpression at 17q in gastric cancer. *Cancer Res.* **62**, 2625–2629 (2002).
25. Q. Hou, Y. H. Wu, H. Grabsch, Y. Zhu, S. H. Leong, K. Ganesan, D. Cross, L. K. Tan, J. Tao, V. Gopalakrishnan, B. L. Tang, O. L. Kon, P. Tan, Integrative genomics identifies *RAB23* as an invasion mediator gene in diffuse-type gastric cancer. *Cancer Res.* **68**, 4623–4630 (2008).
26. K. Sato, G. Tamura, T. Tsuchiya, Y. Endoh, K. Sakata, T. Motoyama, O. Usuba, W. Kimura, M. Terashima, S. Nishizuka, T. Zou, S. J. Meltzer, Analysis of genetic and epigenetic alterations of the PTEN gene in gastric cancer. *Virchows Arch.* **440**, 160–165 (2002).
27. N. Kawamata, S. Ogawa, M. Zimmermann, B. Niebuhr, C. Stocking, M. Sanada, K. Hemminki, G. Yamatomo, Y. Nannya, R. Koehler, T. Flohr, C. W. Miller, J. Harbott, W. D. Ludwig, M. Stanulla, M. Schrappe, C. R. Bartram, H. P. Koeffler, Cloning of genes involved in chromosomal translocations by high-resolution single nucleotide polymorphism genomic microarray. *Proc. Natl. Acad. Sci. U.S.A.* **105**, 11921–11926 (2008).
28. J. G. Park, H. Frucht, R. V. LaRocca, D. P. Bliss Jr., Y. Kurita, T. R. Chen, J. G. Henslee, J. B. Trepel, R. T. Jensen, B. E. Johnson, Y.-J. Bang, J.-P. Kim, A. F. Gazdar, Characteristics of cell lines established from human gastric carcinoma. *Cancer Res.* **50**, 2773–2780 (1990).
29. P. Akiva, A. Toporik, S. Edelheit, Y. Peretz, A. Diber, R. Shemesh, A. Novik, R. Sorek, Transcription-mediated gene fusion in the human genome. *Genome Res.* **16**, 30–36 (2006).
30. E. Rodriguez, P. H. Rao, M. Ladanyi, N. Altorki, A. P. Albino, D. P. Kelsen, S. C. Jhanwar, R. S. Chaganti, 11p13-15 is a specific region of chromosomal rearrangement in gastric and esophageal adenocarcinomas. *Cancer Res.* **50**, 6410–6416 (1990).
31. R. J. Florijn, L. A. Bonden, H. Vrolijk, J. Wiegant, J. W. Vaandrager, F. Baas, J. T. den Dunnen, H. J. Tanke, G. J. van Ommen, A. K. Raap, High-resolution DNA Fiber-FISH for genomic DNA mapping and colour bar-coding of large genes. *Hum. Mol. Genet.* **4**, 831–836 (1995).
32. M. Akhtar, Y. Cheng, R. M. Magno, H. Ashktorab, D. T. Smoot, S. J. Meltzer, K. T. Wilson, Promoter methylation regulates *Helicobacter pylori*-stimulated cyclooxygenase-2 expression in gastric epithelial cells. *Cancer Res.* **61**, 2399–2403 (2001).
33. W. Rzeski, L. Turski, C. Ikonomidou, Glutamate antagonists limit tumor growth. *Proc. Natl. Acad. Sci. U.S.A.* **98**, 6372–6377 (2001).
34. T. Takano, J. H. Lin, G. Arcuino, Q. Gao, J. Yang, M. Nedergaard, Glutamate release promotes growth of malignant gliomas. *Nat. Med.* **7**, 1010–1015 (2001).
35. C. Yang, J. Sudderth, T. Dang, R. G. Bachoo, J. G. McDonald, R. J. DeBerardinis, Glioblastoma cells require glutamate dehydrogenase to survive impairments of glucose metabolism or Akt signaling. *Cancer Res.* **69**, 7986–7993 (2009).
36. J. Y. Kim, B. N. Bae, K. S. Kim, E. Shin, K. Park, Osteopontin, CD44, and NFκB expression in gastric adenocarcinoma. *Cancer Res. Treat.* **41**, 29–35 (2009).
37. C. H. Ooi, T. Ivanova, J. Wu, M. Lee, I. B. Tan, J. Tao, L. Ward, J. H. Koo, V. Gopalakrishnan, Y. Zhu, L. L. Cheng, J. Lee, S. Y. Rha, H. C. Chung, K. Ganesan, J. So, K. C. Soo, D. Lim, W. H. Chan, W. K. Wong, D. Bowtell, K. G. Yeoh, H. Grabsch, A. Boussioutas, P. Tan, Oncogenic pathway combinations predict clinical prognosis in gastric cancer. *PLoS Genet.* **5**, e1000676 (2009).
38. X. Wu, T. Kihara, A. Akaike, T. Niidome, H. Sugimoto, PI3K/Akt/mTOR signaling regulates glutamate transporter 1 in astrocytes. *Biochem. Biophys. Res. Commun.* **393**, 514–518 (2010).
39. O. Zelenaia, B. D. Schlag, G. E. Gochenauer, R. Ganel, W. Song, J. S. Beesley, J. B. Grinspan, J. D. Rothstein, M. B. Robinson, Epidermal growth factor receptor agonists increase expression of glutamate transporter GLT-1 in astrocytes through pathways dependent on phosphatidylinositol 3-kinase and transcription factor NF-κB. *Mol. Pharmacol.* **57**, 667–678 (2000).
40. Y. Fukuda, N. Kurihara, I. Imoto, K. Yasui, M. Yoshida, K. Yanagihara, J. G. Park, Y. Nakamura, J. Inazawa, CD44 is a potential target of amplification within the 11p13 amplicon detected in gastric cancer cell lines. *Genes Chromosomes Cancer* **29**, 315–324 (2000).
41. C. G. Mullighan, S. Goorha, I. Radtke, C. B. Miller, E. Coustan-Smith, J. D. Dalton, K. Girtman, S. Mathew, J. Ma, S. B. Pounds, X. Su, C. H. Pui, M. V. Relling, W. E. Evans, S. A. Shurtleff, J. R. Downing, Genome-wide analysis of genetic alterations in acute lymphoblastic leukaemia. *Nature* **446**, 758–764 (2007).
42. R. Beroukhim, C. H. Mermel, D. Porter, G. Wei, S. Raychaudhuri, J. Donovan, J. Barretina, J. S. Boehm, J. Dobson, M. Urashima, K. T. Mc Henry, R. M. Pinchback, A. H. Ligon, Y. J. Cho, L. Haery, H. Greulich, M. Reich, W. Winckler, M. S. Lawrence, B. A. Weir, K. E. Tanaka, D. Y. Chiang, A. J. Bass, A. Loo, C. Hoffman, J. Prensner, T. Liefeld, Q. Gao, D. Yecies, S. Signoretti, E. Maher, F. J. Kaye, H. Sasaki, J. E. Tepper, J. A. Fletcher, J. Tabernero, J. Baselga, M. S. Tsao, F. Demichelis, M. A. Rubin, P. A. Janne, M. J. Daly, C. Nucera, R. L. Levine, B. L. Ebert, S. Gabriel, A. K. Rustgi, C. R. Antonescu, M. Ladanyi, A. Letai, L. A. Garraway, M. Loda, D. G. Beer, L. D. True, A. Okamoto, S. L. Pomeroy, S. Singer, T. R. Golub, E. S. Lander, G. Getz, W. R. Sellers, M. Meyerson, The landscape of somatic copy-number alteration across human cancers. *Nature* **463**, 899–905 (2010).
43. R. J. DeBerardinis, T. Cheng, Q's next: The diverse functions of glutamine in metabolism, cell biology and cancer. *Oncogene* **29**, 313–324 (2010).
44. P. Nicklin, P. Bergman, B. Zhang, E. Triantafellow, H. Wang, B. Nyfeler, H. Yang, M. Hild, C. Kung, C. Wilson, V. E. Myer, J. P. MacKeigan, J. A. Porter, Y. K. Wang, L. C. Cantley, P. M. Finan, L. O. Murphy, Bidirectional transport of amino acids regulates mTOR and autophagy. *Cell* **136**, 521–534 (2009).
45. C. V. Dang, Rethinking the Warburg effect with Myc micromanaging glutamine metabolism. *Cancer Res.* **70**, 859–862 (2010).
46. A. Okada, H. Takehara, K. Yoshida, M. Nishi, H. Miyake, Y. Kita, N. Komi, Increased aspartate and glutamate levels in both gastric and colon cancer tissues. *Tokushima J. Exp. Med.* **40**, 19–25 (1993).

47. **Funding:** Supported by grants BMRC 05/1/31/19/423, NMRC TCR/001/2007, and institutional funding from Duke-NUS and Cancer Sciences Institute of Singapore. **Author contributions:** J.T. designed and performed the experiments. N.T.D., I.B.T., and C.H.O. analyzed the data. K.R., B.H., H.K.O., S.H.L., S.S.L., and V.C. performed additional experiments. J.W., M.L., and S.Z. performed microarray profiling and sequencing. S.Y.R., H.C.C., D.T.S., and H.A. contributed cell lines and other reagents. O.L.K., C.Y., and N.P. supervised the research. P.T. provided funding and wrote the paper. **Competing interests:** The authors declare that they have no competing interests. As required for research projects funded by the Singapore government, the current work is being evaluated by Exploit Technologies Pte Ltd., the intellectual property arm of the Agency for Science Technology and Research, Singapore, for the possibility of filing a patent.

Submitted 28 June 2010
Accepted 18 March 2011
Published 6 April 2011
10.1126/scitranslmed.3001423

Citation: J. Tao, N. T. Deng, K. Ramnarayanan, B. Huang, H. K. Oh, S. H. Leong, S. S. Lim, I. B. Tan, C. H. Ooi, J. Wu, M. Lee, S. Zhang, S. Y. Rha, H. C. Chung, D. T. Smoot, H. Ashktorab, O. L. Kon, V. Cacheux, C. Yap, N. Palanisamy, P. Tan, *CD44-SLC1A2* gene fusions in gastric cancer. *Sci. Transl. Med.* **3**, 77ra30 (2011).